

Inherent structures enumeration for low-density materials

Frank H. Stillinger

Bell Laboratories, Lucent Technologies, Inc., Murray Hill, New Jersey 07974
and Princeton Materials Institute, Princeton University, Princeton, New Jersey 08544

(Received 14 July 2000; published 27 December 2000)

This paper examines the enumeration of potential energy minima (inherent structures) for attracting particles at number densities below ρ_s , the ‘‘shredding point’’ for amorphous deposits. In this low density regime, typical inherent structures are spatially nonuniform, consisting of dense regions penetrated by irregular void space. Two distinct arguments are advanced concluding independently that in this regime the number $\Omega_1(N, V)$ of distinguishable inherent structures for N particles in volume V has an exponential rise rate with N , $\alpha(\rho)$, that diverges as $\rho \rightarrow 0$. A third argument examines the infinite volume limit and concludes that the asymptotic N dependence of $\ln \Omega_1(N, \infty)$ is dominated by a term proportional to $N \ln N$.

DOI: 10.1103/PhysRevE.63.011110

PACS number(s): 05.20.Jj, 61.20.Gy, 61.43.Gt, 61.43.Hv

I. INTRODUCTION

Rarified, or expanded, solids arise from a wide variety of processes. They involve diverse substances, and they have significant scientific, technological, and commercial applications. Well-known examples include low density silica aerogels [1], polymer foams (e.g., styrofoam) [2], and radiation-damage-expanded and spongy metals [3]. Even the room-temperature gases nitrogen and krypton can be deposited as mesoporous solids on low-temperature substrates [4]. Needless to say, in each of these cases attractive bonding interactions at the atomic or molecular length scale provide the mechanical stability that is observed macroscopically.

The objective of the present paper is to contribute at least some qualitative insight into a difficult underlying statistical enumeration problem for low density matter. Specifically this concerns the counting of the distinguishable ‘‘inherent structures’’ (i.e., mechanically stable arrangements) for a given system of N atoms or molecules in a large volume V . These inherent structures are the minima of the potential energy function $\Phi(\mathbf{r}_1 \cdots \mathbf{r}_N)$ that describes interactions among the N particles at positions $\mathbf{r}_1 \cdots \mathbf{r}_N$ [5]. Inherent structures and their basins of attraction (defined by steepest descent mapping) afford a useful descriptive framework for analyzing a wide range of condensed-matter chemical and physical properties [6]. Prior work has concentrated mostly on systems at high density; the present analysis extends the range of applicability to low density in a sense to be explained below.

For present purposes the constituent particles will be assumed to be spherical, structureless, and all of one species. This produces an obvious economy of notation and explanation. However, the reader should bear in mind that generalization to molecules with internal degrees of freedom, and their mixtures, is straightforward.

A previous investigation [7] has demonstrated that the total number of inherent structures $\Omega(N, V)$ under conditions of constant positive number density $\rho = N/V$ has the following asymptotic behavior in the large system limit:

$$\Omega(N, V) = N! \Omega_1(N, V), \quad (1.1)$$

$$\ln \Omega_1(N, V) \sim \alpha(\rho)N,$$

$$\alpha > 0.$$

The $N!$ factor is the trivial contribution from particle permutations that convert any inherent structure into $N! - 1$ others of identical geometric character. The nontrivial quantity Ω_1 asymptotically displays a simple exponential rise with N for the number of geometrically distinguishable inherent structures. The exponential rise rate α is substance specific, and its indicated density dependence in the low density regime is one of the subjects of the present investigation.

Computer-based analyses of the density dependence of inherent structures for fluids that have been generated by steepest descent on the Φ hypersurface from fluid phases in equilibrium have uncovered a common behavior. This is illustrated schematically in Fig. 1, which plots inherent structure pressure versus density. These analyses have included the Lennard-Jones single component system [8], the SPC/E model for water [9], a fused salt [10], and a set of low-molecular-weight hydrocarbons [11]. Above a characteristic number density ρ_s the inherent structures are spatially homogeneous, while below ρ_s they exhibit fractures, voids, or pores that can be geometrically irregular, and that grow in relative extent as ρ declines. The distinguished point ρ_s, p_s in Fig. 1 represents the state of maximum tension that can be sustained by amorphous inherent structures before they shred into a mechanically weaker spongy medium. In all cases thus far studied, starting from a fluid state at high enough temperature to be in a single phase, ρ_s is less than the triple-point density, and $|p_s|$ is 10^1 to 10^2 times the critical pressure [11,12].

The analysis below concerns only the $0 \leq \rho < \rho_s$ regime, so that the inherent structures encompass substantial void regions. The focus lies in unweighted enumeration of all inherent structures, which therefore is dominated by those underlying the high temperature fluid at the chosen density. Section II presents the first of two arguments (neither of which pretends to be rigorous) that conclude α must diverge as ρ approaches 0. This first argument is based on an approximate assignment of the intrabasin motion freedom of particles in the heterogeneous inherent structures. The sec-

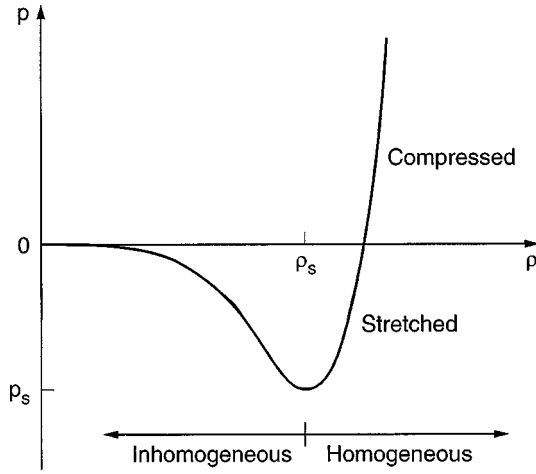


FIG. 1. Schematic plot of isotropic pressure (or tension) vs number density for inherent structures obtained by constant-volume steepest descent mapping on the potential energy hypersurface. The point ρ_s, p_s represents the maximum mechanical strength of amorphous structures; at lower ρ the structures contain irregular pores or fractures, and can only sustain less tension as a result. A similar curve, also with a minimum, describes the mean binding energy of the inherent structures.

ond argument, Sec. III, implements a sequential enforcement scheme to ensure that inherent structures possess the proper backbone connectivity that must be obtained in the presence of attractive interparticle forces.

Section IV examines the companion case of finite- N enumeration of inherent structures in infinite space ($V \rightarrow \infty$). Having established in Secs. II and III that α diverges at $\rho = 0$, it is clear that the number of distinguishable inherent structures must rise faster with N than as a simple exponential. Section IV presents an argument to this effect, a much cruder version of which has appeared earlier [7]. Section V considers the crossover behavior between the small-positive-density, and the zero-density, regimes. Section V also concludes the paper with some discussion, including various points that deserve further examination.

II. LOW POSITIVE DENSITY, FIRST ARGUMENT

Suppose that the quantity α appearing in Eq. (1.1) is known for the number density $\rho_s > 0$ that has been identified in Fig. 1. The mean basin content at this density in the system's $3N$ -dimensional configuration space can be expressed in terms of an effective length d_s applicable to each coordinate, i.e., as d_s^{3N} . The content of the entire configuration space is V^N , so that d_s is determined by

$$V^N = d_s^{3N} N! \exp[\alpha(\rho_s)N], \quad (2.1)$$

or equivalently, using Stirling's formula,

$$\alpha(\rho_s) = \ln \left(\frac{e}{\rho_s d_s^3} \right). \quad (2.2)$$

Considering the fact that the overwhelming majority of the inherent structures at ρ_s are amorphous and spatially uniform, it is reasonable to expect that d_s is comparable to the nearest neighbor separation.

The next step is to consider the effect of reducing the number density ρ to some positive fraction x of ρ_s :

$$\begin{aligned} \rho &= x\rho_s, \\ 0 < x < 1, \end{aligned} \quad (2.3)$$

so that typical inherent structures become “shredded” as described above. The mean basin content can continue to be described by an effective length $d(x)$ for all coordinates, required to satisfy the extension of Eq. (2.2) above:

$$\begin{aligned} \alpha(x\rho_s) &= \ln \left[\frac{e}{x\rho_s d^3(x)} \right], \\ d(1) &= d_s. \end{aligned} \quad (2.4)$$

The behavior of $d(x)$ over the x interval (2.3) must reflect the presence of void space in the inherent structures, with corresponding consequences for $\alpha(\rho)$.

For purposes of helpful context, recall the artificial case for which the system's potential energy function Φ contains only repelling inverse-power pair interactions, but no attractions, and so is immune to shredding of its inherent structures. Elementary scaling arguments [7] establish that α must strictly be independent of ρ , and hence independent of x , so for this case

$$d(x) = x^{-1/3} d(1) \quad (\text{inverse power repulsion}). \quad (2.5)$$

This simple result reflects the uniform dilation of every inherent structure with increasing linear dimension of the volume- V container. Of course this case presents no pressure minimum as shown in Fig. 1, for which attractive interactions are decisive.

An opposing extreme behavior for $d(x)$ hypothetically might emerge in the presence of attractive interactions. In this scenario the entire excess volume generated by reducing x below unity appears as a single, simply connected, macroscopic void. In the large-system limit of interest, only a negligible fraction of the N particles would reside at the surface of this void. The remaining majority would occur locally in high-density neighborhoods just as at ρ_s , and so their freedom for intrabasin displacement as measured by $d(x)$ would be substantially unchanged from $x = 1$:

$$d(x) \cong x^0 d(1) \quad (\text{single macroscopic void}). \quad (2.6)$$

Simulation-based observations of void-containing, low-density inherent structures [8–12] indicate that the actual behavior may lie somewhere between extremes (2.5) and (2.6). The void space typically appears as a tortuous labyrinth, distributed throughout the entire system, with only a microscopic persistence length at any given x [8]. However, the persistence length and fraction of particles at the complicated void surface are expected to grow monotonically as x

declines. Consequently a reduction in x should permit larger intrabasin displacements, and so it becomes reasonable to interpolate Eqs. (2.5) and (2.6) with the following representation:

$$\begin{aligned} d(x) &\cong x^{-q}d(1), \\ 0 &\leq q < 1/3. \end{aligned} \quad (2.7)$$

The lower limit 0 for exponent q should be interpreted to include the possibility of a logarithmic divergence.

Upon inserting Eq. (2.7) into Eq. (2.4) one obtains

$$\alpha(x\rho_s) \cong \alpha(\rho_s) + (3q - 1)\ln x + O(x). \quad (2.8)$$

The coefficient of the negative quantity $\ln x$ is itself negative. The conclusion is that $\alpha(\rho)$ must diverge logarithmically as ρ approaches 0.

III. LOW POSITIVE DENSITY, SECOND ARGUMENT

The volume-spanning porous inherent structures discussed above for $\rho < \rho_s$ are topologically connected by nearest-neighbor-particle attractive contacts. Indeed without such connecting contacts mechanical stability of the inherent structures could not be obtained. This property would appear even if the starting configuration for the steepest descent mapping to an inherent structure were that of a dilute gas. In that case, early stages of the mapping would successively draw close pairs, triplets, quadruplets, . . . , into contact, thus producing an increase in mean cluster size. But the end result cannot be two or more disconnected particle subsets. Realistic interactions always include attractive forces operating at arbitrary distance, however weakly. These attractions inevitably would bring disconnected subsets together to produce a connected whole, leaving much of the system volume vacant. The entire aggregation process, driven by the steepest descent mapping by construction, proceeds without annealing, so the expected outcome virtually always should be an irregular, poorly packed, porous structure.

The emphasis of this second argument is how the connectivity constraint on the final aggregate influences the enumeration of low-density inherent structures. In order to examine the effect of overall connectivity at a coarse-grained level, it is useful to introduce a simple cubic lattice of molecular-scale cells, each of which has a volume v_0 that can be empty or filled by a single particle. This cell-lattice description of connected inherent structures is crude; it obviously suppresses fine details of local particle arrangements in favor of the global connectivity attribute. But since the qualitative character of the low-density $\alpha(\rho)$ behavior should be correctly conveyed, a more fine-grained description should not be required for the present analysis.

An inessential but expedient simplification will be to suppose that the cells are arranged in a macroscopic cube 2^m cells on a side. The total number of cells is

$$M = 2^{3m}, \quad (3.1)$$

which will substantially exceed N in the low-density regime of interest:

$$\begin{aligned} \rho &= N/Mv_0, \\ M &\gg N. \end{aligned} \quad (3.2)$$

It may be useful to consider briefly a specific illustrative example. A realistic macroscopic material sample might contain about one mole of particles, so choose

$$\begin{aligned} N &= 2^{79} \\ &\cong 6.04 \times 10^{23} \\ &\cong N_{Av}. \end{aligned} \quad (3.3)$$

Dispersing this number of particles over the substantially larger number of cells $M = 2^{87}$ produces a gas expanded into a volume $2^8 = 256$ times as large as that required for close packing.

Returning to the general case, the total number of distinguishable arrangements Ω_0 of empty and filled cells regardless of connectivity is given by the elementary combinatorial expression

$$\begin{aligned} \ln \Omega_0 &= \ln \left[\frac{M!}{N!(M-N)!} \right] \\ &= N \left[\left(\frac{M}{N} \right) \ln \left(\frac{M}{N} \right) - \left(\frac{M-N}{N} \right) \ln \left(\frac{M-N}{N} \right) \right] \end{aligned} \quad (3.4)$$

using Stirling's asymptotic formula. In view of strong inequality (3.2), Taylor's expansion through leading order simplifies (3.4) to

$$\ln \Omega_0 = N \left[\ln \left(\frac{M}{N} \right) + 1 \right]. \quad (3.5)$$

In the present coarse-grained context, connectivity will be interpreted in terms of face-sharing between pairs of occupied neighbor cells. Overall, at least one uninterrupted path of such contacts must exist between each pair of occupied cells within a connected system configuration (inherent structure). Edge and vertex sharing will not be considered as contributing to the connectivity. Although the full set of system configurations counted by Ω_0 contains connected configurations, these are but a small fraction of the total. A procedure is required to eliminate the disconnected majority. This will be accomplished, at least approximately, by systematically applying a set of attrition factors to Ω_0 .

On account of the choice of M , Eq. (3.1), the entire cubic cell array can be divided in any of several alternative ways into arrays of nonoverlapping larger cubes, each containing 2^{3j} cells, the number of which is $2^{3(m-j)}$, where $0 \leq j \leq m$. For the specific illustrative example cited above, a relatively dilute system, j would span the range $0 \leq j \leq 87/3 = 29$. This procedure permits a sequential enforcement of connectivity among these sets of larger cubes, starting with $j=0$ and ascending to its upper limit m . At each intermediate stage j one will suppose that the $2^3 = 8$ ($j-1$)-level groupings, which will compose the next-larger cubic grouping, internally and individually possess occupation configurations that

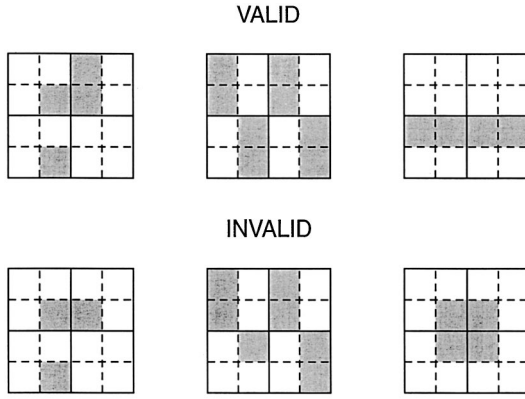


FIG. 2. Typical configurations at the $j=2$ level (in two dimensions), composed of valid $j=1$ subsets (solid outlines), considered during the enforcement of connectivity constraints in Sec. III. Filled cells are gray, empty cells are white. Those patterns labeled “valid” have no necessary disconnections when embedded in the full system, while those labeled “invalid” do. Isolated filled cells at an outer boundary can connect to surrounding portions of the full-system connected configuration.

are consistent with overall system connectivity. The objective then is to assign an attrition factor A_j to each j -level cube expressing the chance that random assembly of those eight smaller cubic groupings, when brought together to form a larger cube, continue to be consistent with overall system connectivity. That they might fail this requirement would stem from absence of necessary connecting particle bridges across faces brought into contact.

Because the j -level cubes by construction do not overlap, their attrition factors A_j are independent of one another. After accounting for these factors and for the numbers of cubic groupings at each level j , the final tally of properly connected configurations takes the form

$$\exp[\alpha(\rho)N + O(1)] = \Omega_0 \prod_{j=0}^m (A_j)^{2^{3(m-j)}}. \quad (3.6)$$

Inclusion of the upper limit $j=m$ in this expression corresponds to imposition of periodic boundary conditions. This use of multiple length scales to analyze a statistical mechanical problem is similar to that introduced by the “renormalization group” approach to critical phenomena [13,14].

Note that at the single-cell level $j=0$, both the empty and the filled states are acceptable, so no attrition occurs. The next level $j=1$, comprising eight contiguous cells in a $2 \times 2 \times 2$ arrangement, presents several distinct possibilities for cell filling, but again none manifestly violate connectivity at this level. Consequently $A_0 = A_1 = 1$. The following level $j=2$ however presents $4 \times 4 \times 4$ arrangements of 64 cells that can either be compatible, or incompatible, with connectivity, so that $0 < A_2 < 1$. Figure 2 illustrates the kinds of possibilities that arise, using the simpler two-dimensional version for ease of visualization, where gray and white, respectively, identify filled and empty cells. Although the first two “valid” examples in the figure are not internally connected through shared faces of occupied cells, they could be

part of a larger connected cluster through external contacts. None of the three “invalid” examples in the figure possess this possibility, and so must suffer attrition.

It is reasonable to invoke a “mean field” approximation to estimate the higher-level attrition factors A_j in Eq. (3.6). For each $j > 1$ it is required that the newly considered cell contacts involve occupancy states that are consistent with the connectivity constraint. The number of cell-pair contacts brought into play upon assembling $2^3 = 8$ ($j-1$)-level groupings into a j -level grouping is 3×2^{2j} . The logarithm of attrition factor A_j should be proportional to this number, but also to the low number density under consideration, to account for filled interfacial cells needing connection to a large cluster at this next higher level, but failing to find it. Therefore set

$$\ln A_j \cong -3C(\rho v_0) \times 2^{2j} \quad (j > 1), \quad (3.7)$$

where C is an appropriate positive constant.

Taking logarithms in Eq. (3.6) and substituting from Eqs. (3.5) and (3.7), one finds

$$\alpha(\rho) \cong -\ln(\rho v_0) + 1 - 3C \sum_{j=2}^m 2^{-j}. \quad (3.8)$$

For the large system limit of interest, m approaches infinity; even for the illustrative example cited above [Eq. (3.3) and the following], m could have reasonably been taken to infinity because of rapidity of convergence of the sum in Eq. (3.8). In either event Eq. (3.8) is equivalent to

$$\alpha(\rho) \cong -\ln(\rho v_0) + 1 - 3C/2. \quad (3.9)$$

Just as was the conclusion for Eq. (2.8) of Sec. II, the implication again is that $\alpha(\rho)$ diverges logarithmically in the low density limit. It should be noted in passing that if both Eqs. (2.8) and (3.9) were qualitatively accurate descriptions of the low density enumeration problem, then consistency would require the following pair of approximate identifications:

$$q \cong 0 \quad (3.10)$$

and

$$\alpha(\rho_s) \cong -\ln(\rho_s v_0) + 1 - 3C/2. \quad (3.11)$$

However both lines of argument admittedly are relatively crude, so Eqs. (3.10) and (3.11) can only be viewed as rough estimates so far as numerical coefficients are concerned. One might note in passing that Eq. (3.10) is nominally consistent with the logarithmic interpretation mentioned in connection with Eq. (2.7) of Sec. II.

IV. FINITE N , INFINITE V

Enumerating distinguishable inherent structures for a finite number of attracting particles in unbounded space constitutes a related, but logically independent, problem to that just considered. The qualitatively consistent results (2.8) and (3.9) imply that the unbounded-space number must rise faster than as a simple exponential function of N . However,

it is not possible without further analysis to infer what the corresponding rise rate should be. An argument will now be presented to resolve this question. It modifies, extends, and strengthens a naïve version that has been published previously [7].

The experimental observation of many kinds of rarified solids as mentioned in the opening paragraph suggests that, when sufficient space is present to allow it, attractive interparticle interactions tend to lead to tenuous inherent structures that are mostly empty space. This view is strengthened by calculations with simple model interactions that demonstrate the existence of vividly noncompact, but mechanically stable, structures [8–12]. When N particles aggregate during steepest-descent mapping from random and dispersed initial positions without the interference of finite boundaries, it is reasonable to expect the typical result to resemble the fractal structures generated by diffusion-limited aggregation processes (DLA) [15,16]. Because so much empty space pervades the expected fractal patterns, one is led to anticipate a far greater set of distinguishable restructuring possibilities in comparison with the high density situation.

Imagine assembling in unbounded space the N -particle inherent structures one particle at a time. At some intermediate stage $1 < N' < N$, the number of distinct inherent structures is given by $\Omega_1(N', \infty)$, the majority of which are open and geometrically irregular. Addition of the next particle could occur anywhere along the contorted surface of the N' -particle cluster. In view of the fractal character expected for the latter, this implies that the number of distinct sites for addition of particle $N' + 1$ should scale with N' as $K(N')^r$, where $K > 0$. Here exponent r is related to the fractal dimension involved, and should be subject to the limits

$$2/3 < r \leq 1, \quad (4.1)$$

thereby interpolating between compact (2/3) and fully extended (1) forms. Consequently one expects

$$\Omega_1(N' + 1, \infty) \cong K(N')^r \Omega_1(N', \infty). \quad (4.2)$$

This relation asserts that each addition has a nonzero chance of spawning a new family tree of larger inherent structures, while still acknowledging that distinct ancestral roots could converge to a common inherent structure. The validity of Eq. (4.4) should not be undermined by the fact that each addition of an attracting particle will produce small local elastic deformations of the prior structure.

Because interest centers on the large- N asymptotic regime, it is appropriate to take logarithms in Eq. (4.4), and to treat N' as a continuous variable. Therefore

$$d \ln \Omega_1(N', \infty) / dN' \cong r \ln N' + \ln K, \quad (4.3)$$

and integrating with respect to N' yields the result

$$\ln \Omega_1(N, \infty) \cong rN \ln N + (\ln K - r)N + L, \quad (4.4)$$

where L is the integration constant. Thus the full enumeration of inherent structures, including permutations and particle symmetries, involves a power of $N!$ that exceeds unity:

$$\ln \Omega(N, \infty) = \ln[(N!)^{1+r}] + O(N). \quad (4.5)$$

The sign of the real integration constant L remains undetermined by the present analysis. In any event Eq. (4.4) verifies that the infinite-space enumeration rises faster with N than as a simple exponential, and so is consistent with conclusions reached in Secs. II and III above.

V. DISCUSSION

The qualitative conclusion, jointly reached in Secs. II and III, that inherent structures tend to be more numerous at low density than at high density, has precedents in the published literature. A special one-dimensional model solved exactly by Haner and Schilling [17] indeed shows just this property. Furthermore, the Gaussian core model in three dimensions possesses an exact convolution property that forces a decline in the number of inherent structures as the system is compressed [18]. Finally, volume dependence of inherent structure appearances and disappearances has been monitored by Malandro and Lacks for a Lennard-Jones-type system, with results that exhibit the same trend [19]. The reader should be aware, however, that each of these three cases did not involve void-containing configurations of the type considered in the present paper. Nevertheless, it is worth noting that the trend toward larger numbers of inherent structures as density declines arises even in spatially uniform particle media.

A crossover range can be identified between the low-positive-density regime examined in Secs. II and III, and the infinite-volume, finite- N regime of Sec. IV. The middle of this crossover range is located formally by equating $\alpha(\rho)N$ from the leading two terms of Eq. (3.9), to the leading two terms of $\ln \Omega_1$ in Eq. (4.4). Let N^* and V^* stand for an N, V pair satisfying this equality. One finds

$$N^* = e(V^*/Kv_0)^{1/(1+r)}, \quad (5.1)$$

and from Eq. (4.1)

$$1/2 \leq 1/(1+r) < 3/5. \quad (5.2)$$

Consequently, as V^* increases toward infinity in this crossover state so too does N^* , but less rapidly. This feature is a consequence of the tenuous fractal nature of the dominating inherent structures that are involved.

The infinite-volume enumeration of inherent structures examined in Sec. IV roughly resembles the enumeration problems for certain families of chemical compounds. A well-known example involves the acyclic family of paraffinic hydrocarbons (alkanes) with the generic chemical formula C_nH_{2n+2} . The number of structural isomers without regard to the presence of chiral carbon centers was enumerated to $n = 40$ many years ago by Henze and Blair [20]. For the present context, the more relevant case involves chiral distinctions. These were considered subsequently in a review by Read [21], with numerical results through $n = 25$. Let $I(n)$ stand for the number of chirality-distinguished isomers with n carbon atoms. The three highest-order results ($n = 23, 24$, and 25) from Ref. [21] fit the following form:

$$\ln I(n) = An \ln n + Bn + C, \quad (5.3)$$

with

$$\begin{aligned} A &= 0.1033, \\ B &= 0.6549, \\ C &= -4.2525, \end{aligned} \quad (5.4)$$

which also well approximates results for all $n > 10$. That A is positive is not too surprising, because the dominant molecular form expected for large n is highly branched and tenuous, just as anticipated in Sec. IV for infinite-volume inherent structures in systems of N attracting particles.

It should be feasible to check at least partially on the

validity of the conclusion of Sec. IV, Eq. (4.4), by computer-implemented direct enumeration of connected clusters on a regular lattice. The simple cubic lattice invoked in Sec. III for the fixed volume case would again be appropriate. Full enumeration of connected clusters up to an order $n \cong 15$ [with fitting to an expression of type (4.4)] seems nominally attainable, though not a trivial task.

One might question whether the free-space count $\Omega(N, \infty)$ of all inherent structures could rise even faster with N than just as a positive power of $N!$, say roughly as $\exp(N^s)$ with $s > 1$. While this possibility cannot yet be rigorously discounted, it seems to lead to an uncomfortable conclusion: large fractal inherent structures could be interconverted in many independent ways by arbitrarily small distortions. Further study of this aspect of the enumeration problem is clearly warranted.

-
- [1] J. Fricke, *Sci. Am.* **258**, 92 (1988).
 [2] J. A. Brydson, *Plastics Materials*, 5th ed. (Butterworths, London, 1989), pp. 426–430.
 [3] *Radiation Effects*, Metallurgical Society Conferences, edited by W. F. Sheely (Gordon and Breach, New York, 1967), Vol. 37; T. A. Engh, *Principals of Metal Refining* (Oxford University Press, Oxford, 1992), p. 154.
 [4] V. Kiryukhin, B. Keimer, R. E. Boltnev, V. V. Khmelenko, and E. B. Gordon, *Phys. Rev. Lett.* **79**, 1774 (1997).
 [5] F. H. Stillinger and T. A. Weber, *Phys. Rev. A* **28**, 2408 (1983); F. Sciortino, W. Kob, and P. Tartaglia, *Phys. Rev. Lett.* **83**, 3214 (1999).
 [6] F. H. Stillinger and T. A. Weber, *J. Chem. Phys.* **81**, 5095 (1984); *Phys. Rev. B* **31**, 5262 (1985); *J. Phys. Chem.* **91**, 4899 (1987); L. J. Root, *J. Chem. Phys.* **93**, 4364 (1990); H. Tanaka and K. Nakanishi, *ibid.* **95**, 3719 (1991); F. L. Somer, Jr., G. S. Canright, T. Kaplan, K. Chen, and M. Mosteller, *Phys. Rev. Lett.* **79**, 3431 (1997); D. J. Wales and H. A. Scheraga, *Science* **285**, 2210 (1999).
 [7] F. H. Stillinger, *Phys. Rev. E* **59**, 48 (1999).
 [8] S. Sastry, P. G. Debenedetti, and F. H. Stillinger, *Phys. Rev. E* **56**, 5533 (1997).
 [9] C. J. Roberts, P. G. Debenedetti, and F. H. Stillinger, *J. Phys. Chem. B* **103**, 10 258 (1999).
 [10] R. A. LaViolette, J. L. Budzien, and F. H. Stillinger, *J. Chem. Phys.* **112**, 8072 (2000).
 [11] M. Utz, P. G. Debenedetti, and F. H. Stillinger (unpublished).
 [12] P. G. Debenedetti, F. H. Stillinger, T. M. Truskett, and C. J. Roberts, *J. Phys. Chem. B* **103**, 7390 (1999).
 [13] L. P. Kadanoff, *Physics* (Long Island City, N.Y.) **2**, 263 (1966).
 [14] M. E. Fisher, *Rev. Mod. Phys.* **70**, 653 (1998).
 [15] T. A. Witten and L. M. Sander, *Phys. Rev. Lett.* **47**, 1400 (1981).
 [16] P. Meakin, in *Phase Transitions and Critical Phenomena*, edited by C. Domb and J. L. Lebowitz (Academic, New York, 1988), Vol. 12.
 [17] P. Haner and R. Schilling, *Europhys. Lett.* **8**, 129 (1989).
 [18] F. H. Stillinger and D. K. Stillinger, *Physica A* **244**, 358 (1997).
 [19] D. L. Malandro and D. J. Lacks, *J. Chem. Phys.* **107**, 5804 (1997).
 [20] H. R. Henze and C. M. Blair, *J. Am. Chem. Soc.* **53**, 3077 (1931).
 [21] R. C. Read, in *Chemical Applications of Graph Theory*, edited by A. T. Balaban (Academic, New York, 1976), Chap. 4, pp. 44–45, Table II.